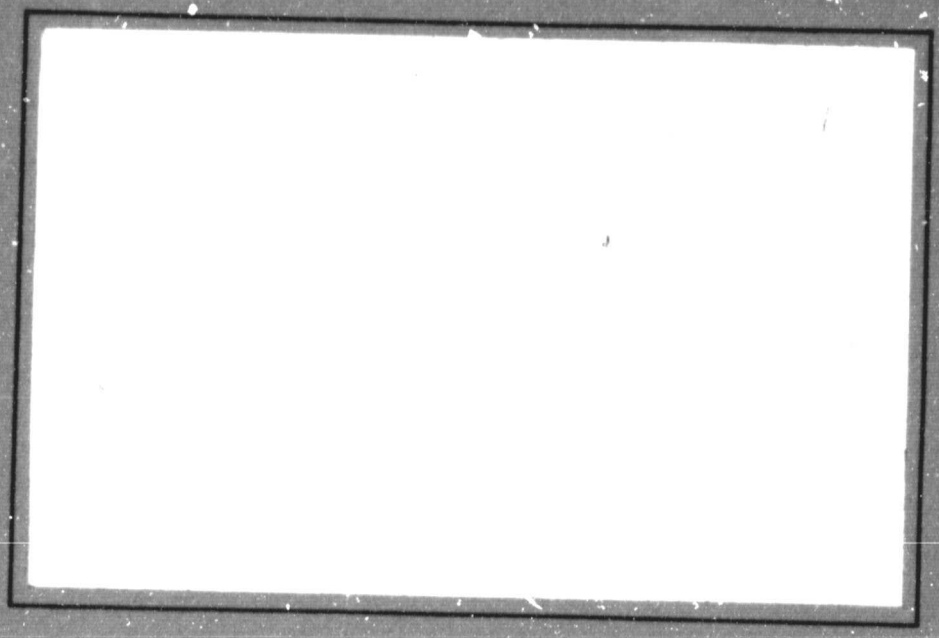

(NASA-CR-175353) SURFACE ANALYSIS IN COMPOSITE BONDING Semiannual Technical Report (Virginia Polytechnic Inst. and State Univ.) 39 p HC A03/MF A01 CSCL 11D

N84-16264

Unclas
G3/24 18251

Virginia Polytechnic Institute and State University

Chemistry Department

Blacksburg, Virginia 24061

SEMI-ANNUAL TECHNICAL REPORT

SURFACE ANALYSIS IN COMPOSITE BONDING

by

D. L. Messick and J. P. Wightman

Prepared for

National Aeronautics and Space Administration

December, 1983

Grant NAG 1-343

NASA-Langley Resarch Center
Hampton, Virginia 23665
Materials Division
Donald J. Progar

Department of Chemistry
Virginia Polytechnic Institute and State University
Blacksburg, Virginia 24061

TABLE OF CONTENTS

SURFACE ANALYSIS IN COMPOSITE BONDING

I. INTRODUCTION

There is increasing use of graphite fiber reinforced composites for example in the aircraft industry. There is a concomitant increase in interest of adhesively bonding these composites. A SEM photomicrograph of a typical graphite fiber reinforced composite surface is shown in Figure 1. It is the detailed analysis of this kind of surface which is the primary objective of this research. However, it is recognized that not only is the composite surface of interest but also the characterization of the fibers themselves and the interaction between the fibers and the matrix. This report will discuss surface analysis results for graphite fibers and then for graphite reinforced composites prior to adhesive bonding and following fracture of lap shear samples.

II. GRAPHITE FIBERS

We have reported earlier (1) a study of coated and uncoated graphite fibers. A description of the fibers studied is given in Table I. Representative SEM photomicrographs of HTS-2 fibers and HMS fibers are shown in Figure 2. Striations are noted for the HMS fibers in contrast to the smooth surface of the HTS-2 fibers.

A wide scan ESCA spectrum of HTS graphite fibers is shown in Figure 3. The major photopeaks are assigned to carbon and oxygen. A minor N 1s photopeak is also observed. These fibers have quite clean surfaces. Three narrow scan ESCA spectra for the C 1s, O 1s and N 1s photopeaks are shown in Figure 4 for Thornel 300 fibers. A summary of the ESCA results for the different graphite fibers are shown in Table II. The binding energies for all

the C 1s and N 1s photopeaks are fairly constant. The atomic percentages (AP) of both oxygen and nitrogen are also listed in Table II; the balance is due to carbon. Significant differences are noted in both the C/O and C/N ratios for the different fibers. The HTS-2 fibers have the highest carbon content as gauged by the high values of both sets of atomic ratios. The surface composition of uncoated and epoxy coated Thornel 300 fibers varies significantly. The C/N ratio of Celion 6000 increases on rinsing with methyl ethyl ketone suggesting some removal of the polyimide finish from these particular fibers.

The ESCA spectra of Courtaulds AS carbon fibers reported by Waltersson (2) are shown in Figure 5. Trace amounts of sulfur, chlorine, sodium and silicon were noted and are commonly observed residuals of PAN-based carbon AS fibers. The presence of calcium had not been reported previously but its source was not identified. Brewis et al. (3) used ESCA to detect changes in surface composition resulting from different oxidation pretreatments of acrylic fibers carbonized at 1600°C as shown in spectra A - D in Figure 6. Photopeaks A and B in the unresolved O 1s is doublet of the untreated fiber are assigned to at least two different oxygen species. The lower binding energy component (Photopeak B) is more predominant in the oxidized fibers. Hopfgarten (4) demonstrated using ESCA that oxidation of Courtaulds HM-S carbon fibers is limited to <50 nm by ion etching. The ESCA spectra before and after etching are shown in Figure 7. The original surface has a significant O 1s photopeak but oxygen does not appear on the surface which has been ion etched to a depth of 50 nm.

The surface energy of graphite fibers has been studied thermodynamically in an extensive series of gas adsorption and contact angle measurements by Drzal and co-workers (5,6). An analysis (5) of the adsorption of krypton on

untreated PAN fibers gives a surface area of the fibers of about 0.5 m^2/g. A detailed analysis of contact angles of liquids against graphite fibers was made (6) to estimate the polar and dispersion components of the surface energy of untreated and surface treated fibers. The equation below was used to calculate γ_S^D and γ_S^P the dispersion and polar components of the surface energy of the fiber, resp.

$$\gamma_L (1+\cos\theta)/2 \, (\gamma_L^D)^{1/2} = (\gamma_S^D)^{1/2} + (\gamma_S^P)^{1/2} \, (\gamma_L^P/\gamma_L^D)^{1/2}$$

Here, contact angles (θ) of liquids having known γ_L^D and γ_L^P values are measured against the fiber. Selected results are listed in Table III. The PAN fibers designated 'A' and 'HM' were graphitized at 1500° and 2600°C, resp. The designations 'U' and 'S' mean untreated and surface treated to promote matrix adhesion by Hercules, Inc. The surface treatment of either type fiber leads to a marked increase in the polar component γ_S^P of the surface energy and hence to an increase in the total surface energy γ_S^T. In a separate series of experiments, the concentration of oxygen in the fiber surface was calculated from the ESCA spectra. The correspondence of the results of the macroscopic contact angle and the microscopic ESCA measurements is illustrated in Figure 8. Here the γ_S^P values increase with an increase in the surface oxygen content of the fibers.

The significance of measurements of surface composition in composite adhesion is summarized succinctly in Figure 9 where interlaminar strengths of carbon fiber-based composites are plotted against the density of acidic groups on the fiber surface (7). An increase in interlaminar strength results from an increase in the number of surface acidic groups. Presumably, the higher

strengths result from enhanced adhesion between acidic groups on the fiber surface and the matrix. Such results bespeak the importance of careful surface characterization not only of the composite but of the fibers themselves.

III. GRAPHITE FIBER REINFORCED COMPOSITES

The analysis of graphite composite surfaces is prefaced by reference to the work of Parker and Waghorne (8). The results shown in Figure 10 demonstrate the marked dependence of the lap shear strengths of carbon fiber-reinforced composites on the concentration of fluorine on the composite surface. The higher the surface fluorine concentration, the lower the lap shear strength. Different adhesives show varying dependencies with a room temperature curing modified epoxy paste being the most sensitive.

A. Composite Fabrication and Surface Pretreatment

Celion 6000/LARC - 160 composites were fabricated by Rockwell International. Particulars of the fabrication process are shown in Figures 11-13 and properties of the fabricated composite panels are given in Table IV. A SEM photomicrograph of the fabricated composite surface before any pretreatment is shown in Figure 14. The composite panels were subsequently pretreated in a variety of different ways including mechanical abrasion, chemical etching and light irradiation by the Flashblast® process. Details of the pretreatment processes have been reported (9, 10).

B. Composite Surface Characterization Prior to Bonding

SEM photomicrographs of the composite surfaces following a SiC handsand and the Flashblast® process are shown in Figures 15 and 16 resp. Some matrix removal but minimal fiber damage is noted in Figure 15 for the SiC

handsand. The composite surface is altered clearly by the Flashblast® process as seen in Figure 16. SEM photomicrographs for the chemically etched composite surfaces were quite similar to the untreated surface. Progar (11) has done an extensive SEM study of the pretreated composite surfaces.

Selected ESCA results of the composite surfaces are summarized in Table V. The binding energy (in ev) and atomic fraction of each major photopeak is listed. Fluorine was detected at varying levels on most of the composite surfaces. A delaminated surface showed a minimal fluorine signal suggesting that fluorine was introduced only onto the external composite surface during the fabrication process presumably by contact with the teflon coated glass fabric (3TLL) shown in Figures 11 and 12. Carbon, nitrogen and oxygen are expected since a polyimide matrix resin was used. Atomic fraction ratios are listed in Table VI. The O/C and N/C ratios are fairly constant for the untreated, delaminated, mechanically abraded and chemically etched composite surfaces. However, large differences are noted in the F/C ratio of these same surfaces. Mechanical abrasion reduced the fluorine content whereas chemical etching was ineffective in reducing the fluorine content. The Flashblast® process not only eliminated the surface fluorine but also oxygen and nitrogen as gauged by the low values for the three atomic ratios. Thus, the Flashblast® process results in a carbonized surface.

ESCA results obtained during ion sputtering of the untreated composite surface are shown in Figure 17. Sputter time on the abscissa is directly proportional to depth. Thus, the fluorine signal decreases quickly or alternately stated the fluorine is restricted to the topmost surface of the composite. This conclusion is consistent with the minimal fluorine signal observed for the surface resulting from delamination.

Reilley and co-workers (11) have demonstrated convincingly the utility of doing ESCA on derivatized surfaces to determine the types of functional groups

present on the surfaces. Some derivatization reactions are shown in Table VII with the surface functional group on the left and the expected surface group after reaction with the derivatizing agent on the right. We have applied this elegant technique for the first time to composite surfaces. Preliminary results are shown in Figure 18. Spectra A and B are the F 1s and Hg 4f7 and 4f5 photopeaks, resp., after derivatizing reactions [3] and [5] (see Table VII) on the as-received composite. The results indicate that both (COOH) and (C=C) groups are present on the composite surface. Work is in progress to further document these assignments of surface functional groups. In complementary experiments, Young, Stein and Chang have reported(12) assignment of surface functional groups on similar composite surfaces using diffuse reflectance FT-IR.

Critical surface tensions (γ_c) of the composites were obtained from measured contact angles of liquids against the composites using the Zisman approach (13). The γ_c values are listed in the last column of Table VI where significant differences were noted for the different composite surfaces. Again, the correspondence between the results of the macroscopic contact angle measurements and the microscopic ESCA results is demonstrated in Figure 19. Here, the composite surfaces with the lower critical surface tensions have the higher surface fluorine concentrations. It would be expected based on Parker and Wanghorne's results (8) discussed above (see Figure 10) that the lap shear strengths of the untreated composite having a high surface fluorine concentration would be significantly lower than for pretreated surfaces with a lower surface fluorine concentration.

C. Composite Surface Characterization Following Lap Shear Fracture

The Celion 6000/LARC 160 composites panels were bonded with the epoxy FM 34B-18 adhesive . Lap shear strengths of unaged and thermally aged samples

are given in Table VIII. The untreated composite can be compared to a mechanically abraded (SiC handsand), a chemical etch (hydrazine hydrate) and the Fflashblast® process. Surprisingly, there is no apparent effect of composite pretreatment prior to bonding on lap shear strength. That is, the lap shear strength of the untreated composite is equivalent to the lap shear strengths for the three pretreated surfaces. At first glance, these results may appear to be inconsistent with those of Parker and Wanghorne (8). However, the results in Fig. 10 show that for some adhesives, surface fluorine concentrations in excess of 50% are necessary before a significant reduction of lap shear strength occurs. Presumably, the lap shear strength of Celion 6000 composite with a LARC-160 polyimide matrix is not strongly dependent on surface fluorine concentrations at least up to 30%.

A much reduced fluorine signal is noted in Table VIII for the fracture surface of all samples compared to the pretreated but unbonded sample. This result suggests either migration of the fluorine-containing species out of the fracture region or that fracture occurred away from the original bonding surfaces. Further work is necessary to distinguish between these two possibilities.

The lap shear strengths of the thermally aged samples also listed in Table VIII are significantly lower by a factor of two than for the unaged (control) samples. It may be significant that in every case the fluorine concentration in the fracture surface is greater for the aged than for the unaged sample. It is not clear whether the presence of fluorine resulted in the lower lap shear strengths of the thermally aged samples.

IV. SUMMARY

A significant fluorine signal was observed by ESCA on the as-received Celion 6000/LARC-160 composite surface prior to pretreatment. Only a trace

fluorine signal is noted on a delaminated surface of the same as-received sample. This result indicates that fluorine is introduced probably by contact with the Teflon coated glass fabric during the fabrication step. Chemical pretreatment was the least effective method of removing surface fluorine while the Flashblast® process reduced the fluorine signal to trace levels. Critical surface tensions of the pretreated composites were determined from measured contact angles. Low critical surface tensions were characteristic of composite surfaces having high surface fluorine concentration as determined by ESCA.

The lap shear strength of the composites bonded with epoxy was independent of the type of pretreatment and in turn the surface fluorine concentration. In contrast, the lap shear strength of thermally aged bonded composites was about one-half that of the control samples. There was a significant increase in the surface fluorine concentration on the fracture surfaces of the thermally aged samples. The effect, if any, of this fluorine on the lap shear strength of thermally aged composites was not established.

The ESCA results and contact angle measurements produced information on the surface contamination as a result of fabrication techniques which may provide answers to the strength and durability of adhesively bonded composites. These techniques have been shown to be capable of providing valuable information with respect to surface analysis of pretreated composites prior to adhesive bonding and following lap shear fracture.

V. ACKNOWLEDGEMENT

We thank Frank Cromer of the Poly-Scientific Company for the ESCA analysis and Dr. James Jen of Owens-Corning Fiberglas for the ESCA depth profiling analysis.

VI. REFERENCES

1. W. Chen and J. P. Wightman, in "Abstracts of 14th Biennial Conference on Carbon", p. 107, University Park, PA (1979).
2. K. Waltersson, Fibre Science and Technology, 17, 289 (1982).
3. D. M. Brewis, J. Comyn, J. R. Fowler, D. Briggs and V. A. Gibson, Fibre Science and Technology, 12, 41 (1979).
4. F. Hopfgarten, Fibre Science and Technology, 12, 283 (1979).
5. L. T. Drzal, in "Treatise on Adhesion and Adhesives, Vol. 5, R. L. Patrick, Ed., pp 21 ff, Marcel Dekker, New York ( ).
6. G. E. Hammer and L. T. Drzal, Applications of Surface Science, 4, 340 (1980).
7. P. Ehrburger and J. B. Donnet, Phil. Trans. Royal Soc. London, A294, 495 (1980).
8. B. M. Parker and R. M. Waghorne, Composites, 280 (1982).
9. D. L. Messick, D. J. Progar and J. P. Wightman, in Proc. 15th Natl. SAMPE Techn. Conf., M. Smith, Ed., pp 170-189, SAMPE, Azusa, CA (1983).
10. D. L. Messick, D. J. Progar and J. P. Wightman, NASA TM 85700, NASA-Langley Research Center, Hampton, VA (1983).
11. D. S. Everhart and C. N. Reilley, Anal. Chem., 53, 665 (1981).
12. P. R. Young, B. A. Stein and A. C. Chang, SAMPE Preprints, 28, 824 (1983).
13. W. A. Zisman in "Contact Angle, Wettability and Adhesion", Adv. Chem. Series #43, R. F. Gould, Ed., pp 1-51, Am. Chem. Soc., Washington (1964).

TABLE I

DESCRIPTION OF GRAPHITE FIBERS

Graphite Fibers	Description
HMS	Batch No. 32-2 No surface finish
HTS-2	Batch No. 94-1 No surface finish
Celion 6000	Lot No. HTH-7-7711 1.2% polyimide finish
Thornel 300	Grade WYP 30% Epoxy finish (UC 309)
NASA-2	CG-3 fiber coated with styrene/maleic anhydride
NASA-3	HTS fiber coated with nadic anhydride

TABLE II

ESCA ANALYSIS OF GRAPHITE FIBERS

Fiber	C 1s BE(eV)	C 1s AP	O 1s BE(eV)	O 1s AP	N 1s Be(eV)	N 1s AP	C/O	C/N
1. HMS	(284.0)	88.6	532.4	9.7	399.5	1.7	9.	52.
2. HTS-2	(284.0)	92.9	532.2	6.7	399.4	0.4	14.*	232.*
3. Thornel 300	(284.0)	85.0	532.3	13.4	399.8	1.6	6.	53.
4. Thornel 300 Epoxy finish	(284.0)	72.4	531.9	23.1	399.0	4.5	3.	16.
5. Celion 6000 Polyimide finish	(284.0)	85.3	531.4	11.8	398.4	2.9	7.	29.
6. Celion 6000 MEX rinse	(284.0)	85.3	531.8	13.0	399.0	1.7	7.	50.
7. NASA-2	(284.0)	83.0	531.6	16.0	398.6	1.0	5.	83.
8. NSAS-2 Toluene rinse	(284.0)	84.2	532.0	14.5	399.4	1.3	6.	65.
9. NASA-3	(284.0)	81.0	531.8	17.6	399.1	1.4	5.	58.
10. NASA-3 Toluene rinse	(284.0)	82.0	531.6	16.4	398.6	1.6	5.	51.
					Average		6±1	51±13

*Values not included in average

TABLE III

POLAR, DISPERSIVE AND TOTAL SURFACE FREE ENERGY OF GRAPHITE FIBER SURFACES

Fibers	Surface free energy (mJ/m^2)		
	γ_S^P	γ_S^D	γ_S^T
"as received"			
AU	23.6	27.4	51.0
AS	30.0	26.4	56.4
HMU	8.1	33.0	41.1
HMS	20.7	28.2	48.9

TABLE IV

PROPERTIES OF CELION 6000/LARC-160 COMPOSITE[a]

Panel No.	Tg(°C)	Average Thickness(mm)	Specific Gravity	V_F %	Void %
1	344 (651°F)	2.2 (0.086 in)	1.57	59	0.1
2	332 (629°F)	2 0 (0.079 in)	1.58	61	<1.0

[a] $(0,0,0,+30,-30,+30,-30)_S$ ply orientation.

TABLE V

ESCA ANALYSIS OF COMPOSITES

Sample No.	Sample Pretreatment	Photopeak F 1s	O 1s	N 1s	C 1s	
1A	As-received	689.0	531.8	399.8	(284.6)	B.E.(eV)
		0.19	0.11	0.030	0.66	A.F.
1B	Delaminated	688.8	532.4	400.2	(284.6)	
		0.002	0.11	0.020	0.86	
5	600 SiC Handsand	689.4	532.2	400.2	(284.6)	
		0.025	0.13	0.020	0.80	
9	Concd. H_2SO_4 + 30% H_2O_2	689.2	532.0	400.0	(284.6)	
		0.19	0.12	0.020	0.66	
11	Flashblast #2	-	532.6	-	(284.6)	
		NSP	0.053	NSP	0.93	

NSP - no significant peak

TABLE VI

ESCA ATOMIC RATIOS AND CRITICAL SURFACE TENSIONS OF COMPOSITES

Sample No.	Atomic Fraction Ratio			Critical Surface Tension (mJ/m^2)
	F/C	O/C	N/C	
1A	0.29	0.17	0.045	23.
1B	0.0023	0.13	0.023	--
5	0.031	0.16	0.025	35.
9	0.29	0.18	0.030	31.
11	<0.001	0.057	<0.001	40.

TABLE VII

DERIVATIZATION REACTIONS

Reaction		Product
$\vdash NH_2$	1 $\xrightarrow{C_6F_5CHO}$	$\vdash N{=}CHC_6F_5$
$\vdash CO_2H$	2 $\xrightarrow{(CF_3CO)_2O}$	$\vdash COOCOCF_3$ $\vdash O_2CCF_3$
$\vdash CO_2H$	3 $\xrightarrow[2)\ C_6F_5CH_2Br]{1)\ KOH(ROH)}$	$\vdash CO_2CH_2C_6H_5$
$\vdash C{=}O$	4 $\xrightarrow{C_6F_5NHNH_2}$	$\vdash C{=}NNHC_6F_5$
$\vdash C{=}C{-}$	5 $\xrightarrow[Cl_3CH_2OH]{Hg(CF_3CO_2)_2}$	$\vdash C(-Hg(CF_3CO_2))-C(-OCH_2CCl_3)$

TABLE VIII

LAP SHEAR STRENGTHS OF THERMALLY AGED ADHESIVELY BONDED COMPOSITES

Sample Pretreatment	$(F/C)_o$	Exp. Temp (°F)	LSS (psi)	$(F/C)_f$
as-received	0.29	CONTROL	3045	0.025
as-received	0.29	450	1245	0.15
600 SiC Handsand	0.031	CONTROL	2940	0.020
600 SiC Handsand	0.031	450	1445	0.034
$NH_2NH_2 \cdot H_2O$	0.31	CONTROL	3080	0.018
$NH_2NH_2 \cdot H_2O$	0.31	CONTROL	3080	0.011
$NH_2NH_2 \cdot H_2O$	0.31	450	1220	0.079
$NH_2NH_2 \cdot H_2O$	0.31	450	1220	0.090
Flashblast® #2	<0.001	CONTROL	2935	--
Flashblast® #2	<0.001	450	1280	--

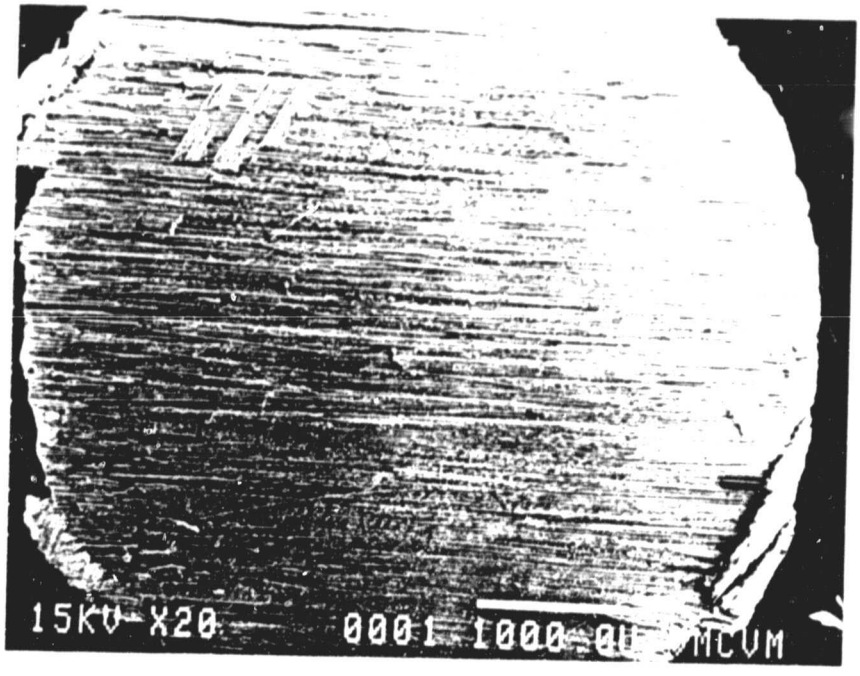

Figure 1. SEM photomicrograph of graphite fiber-reinforced polyimide composite.

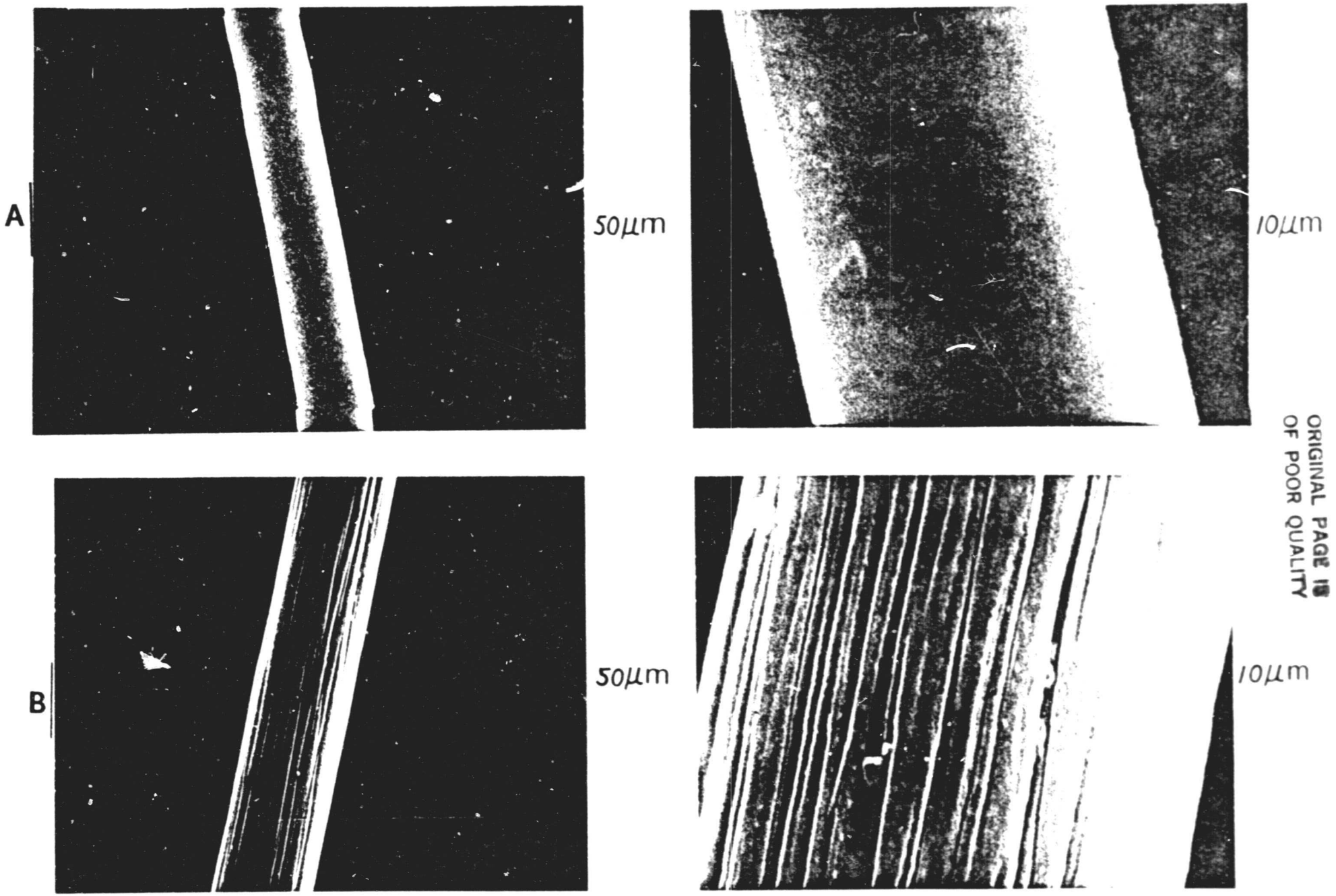

Figure 2. (a) SEM photomicrographs of HTS-2 graphite fiber.

(b) SEM photomicrographs of HMS graphite fiber.

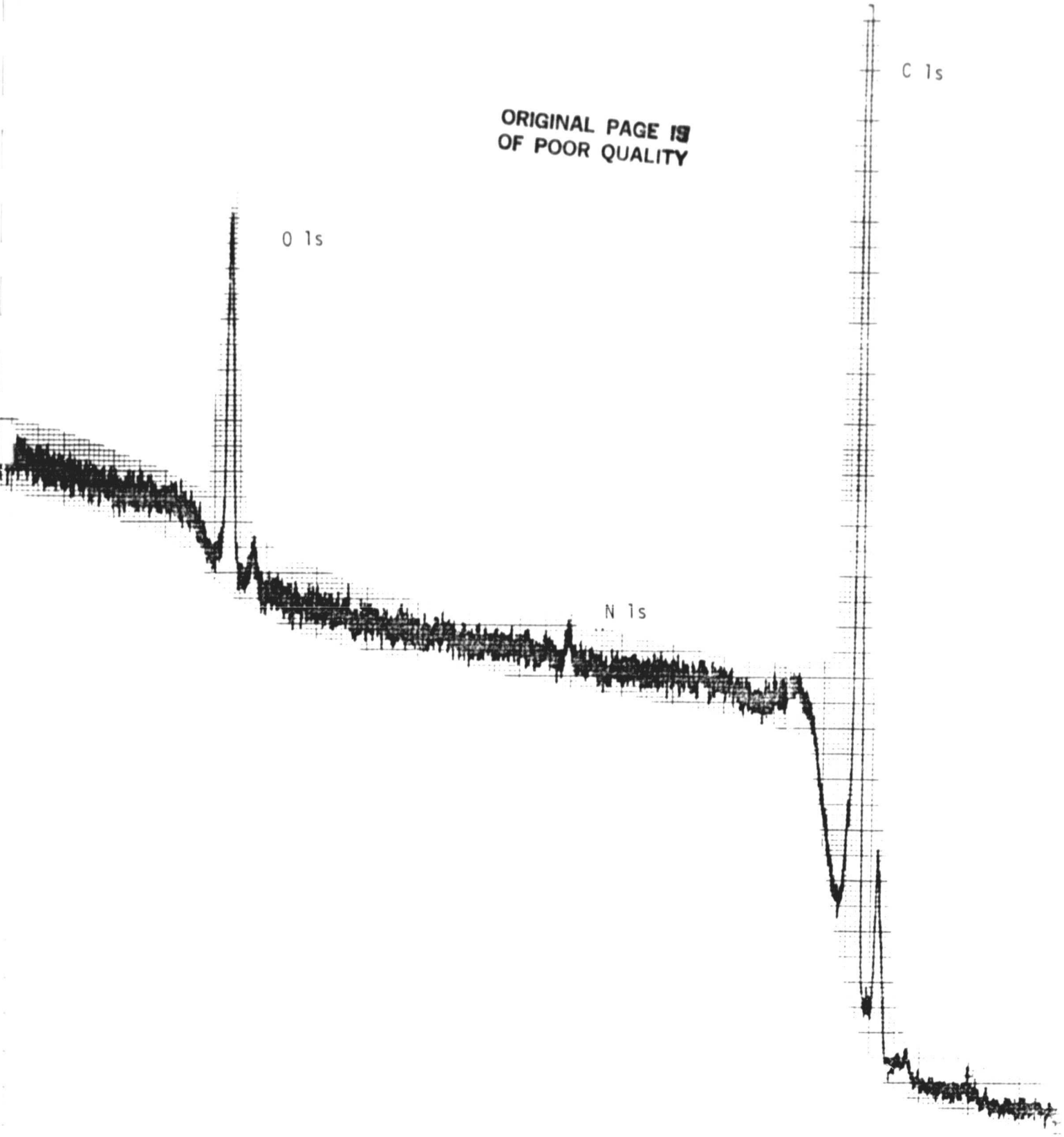

Figure 3. Wide scan ESCA spectrum of HTS graphite fibers.

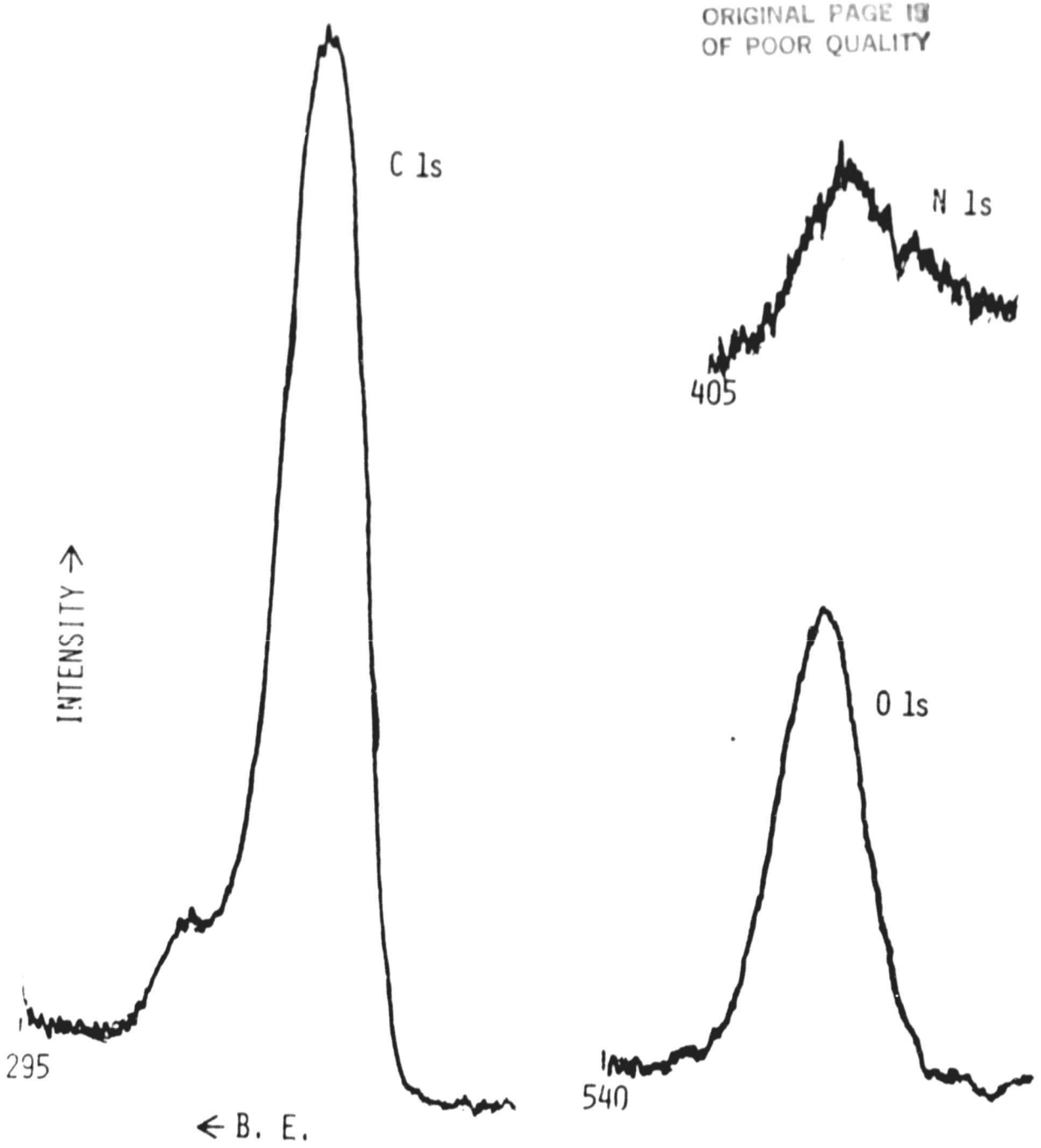

Figure 4. Narrow scan ESCA spectra of Thornel 300 graphite fibers.

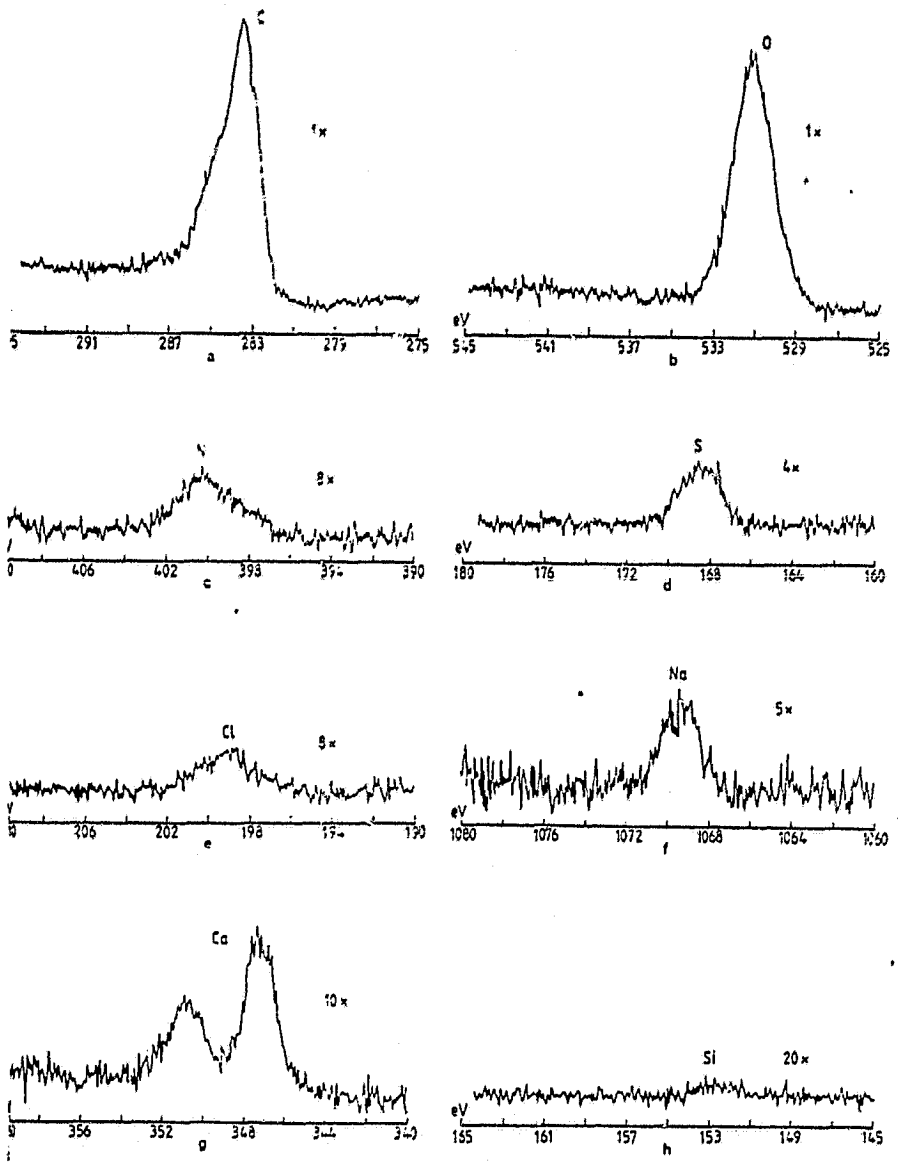

Figure 5. ESCA spectra of Courtaulds AS carbon fibers (2).

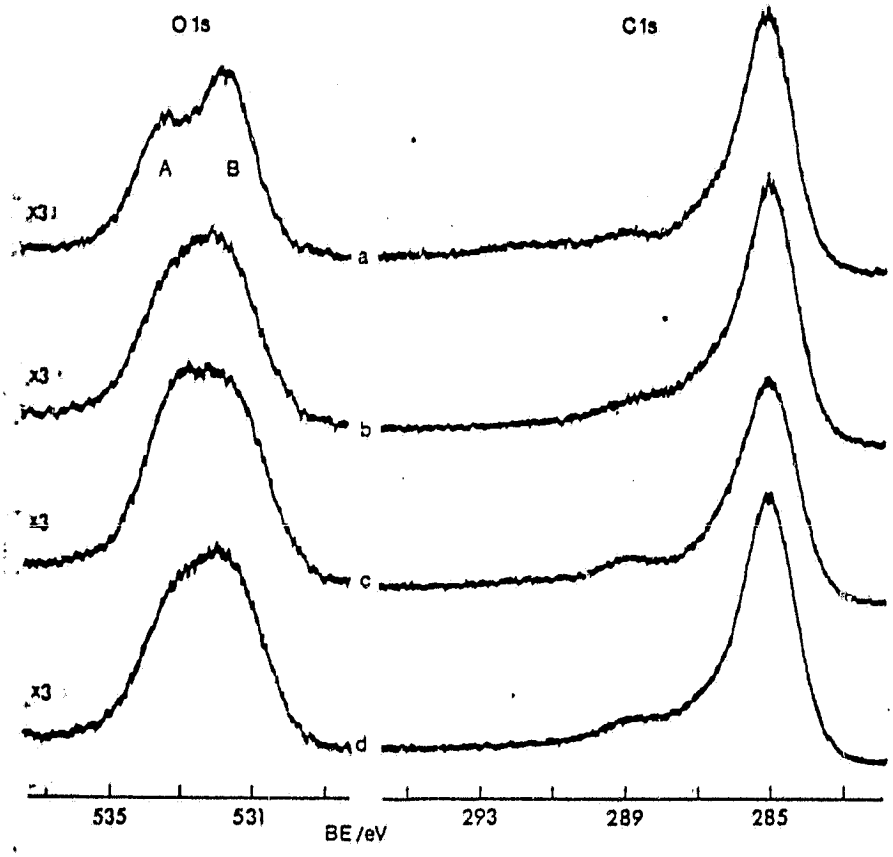

Figure 6. ESCA spectra of pretreated acrylic fibers carbonized at 1600°C (3).

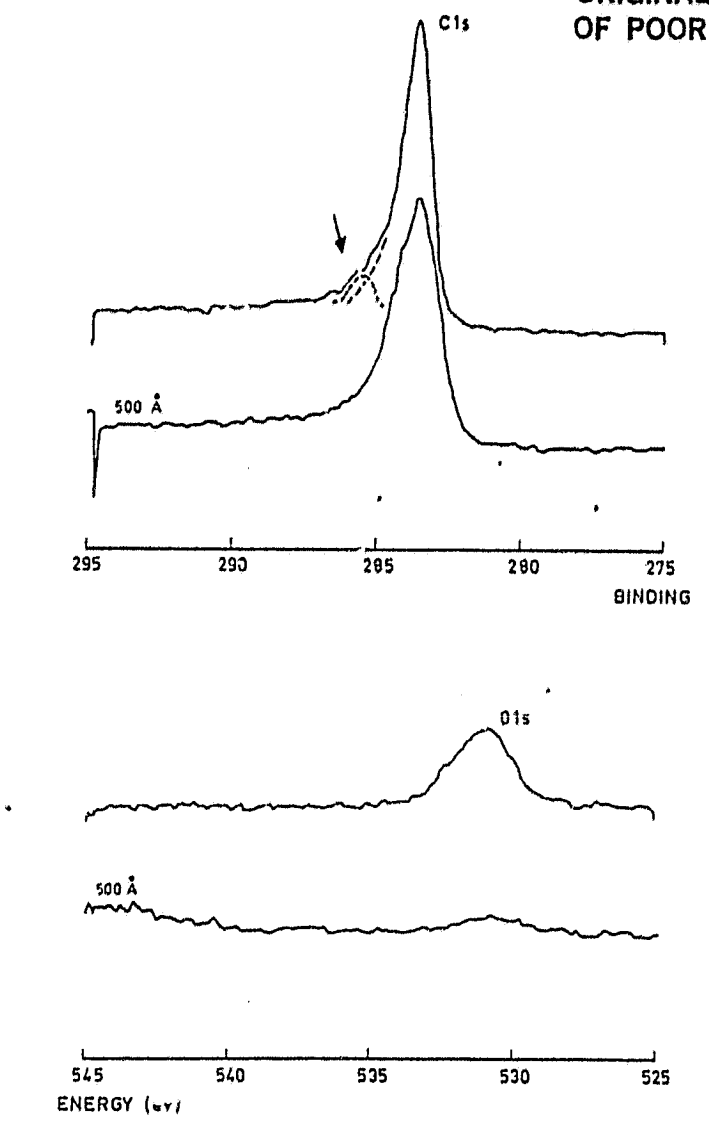

Figure 7. ESCA spectra of Courtaulds HM-S carbon fibers before and after ion etching (4).

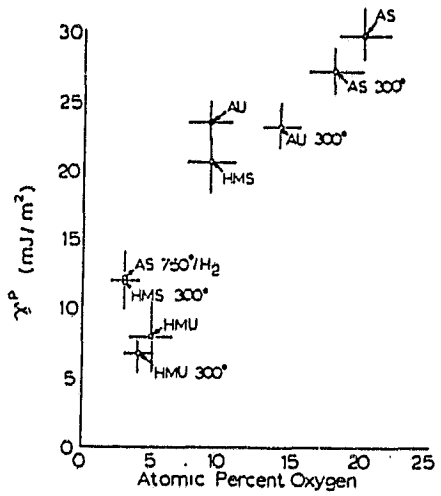

Figure 6. Polar component of the surface energy of PAN fibers as a function of surface oxygen content (6).

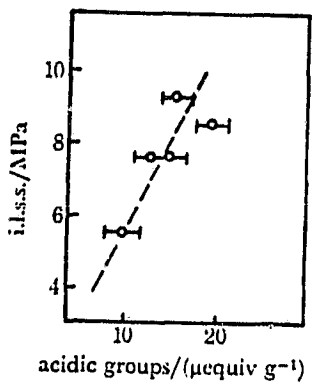

Figure 9. Interlaminar strengths of carbon fiber-based composites as a function of the density of acidic groups on the fiber surface (7).

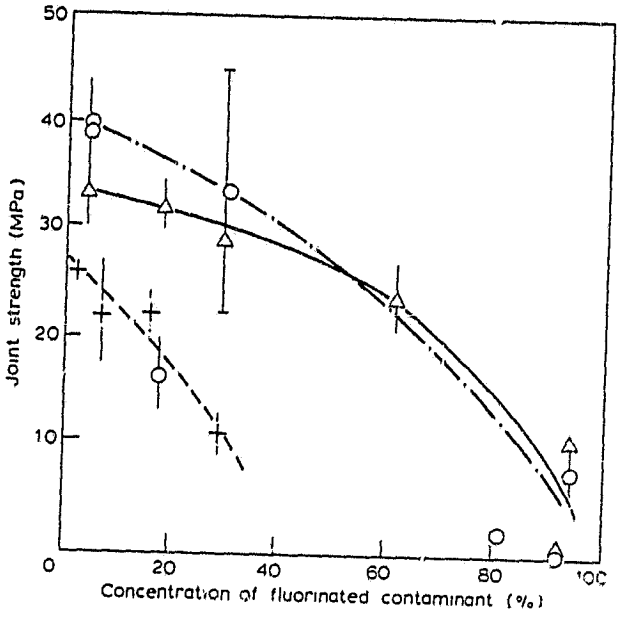

Figure 10. Lap shear strengths of carbon fiber-reinforced composites as a function of surface fluoride content (8).

(a) VACUUM BAG LAYUP

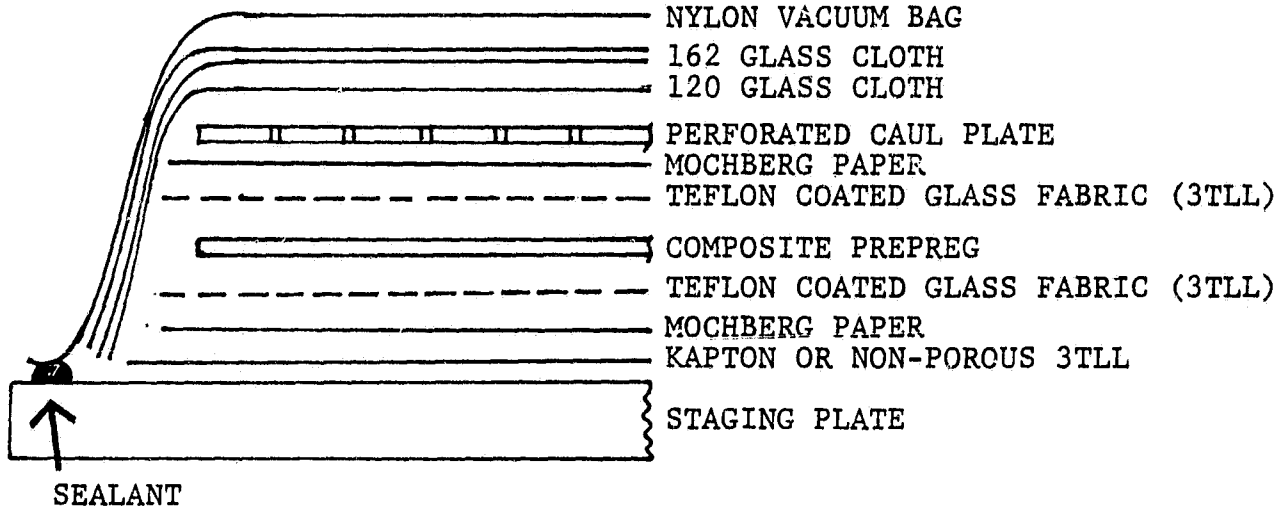

(b) STAGING CONDITIONS

1. APPLY 12.7cm (5in) Hg VACUUM AND HOLD FOR FULL CYCLE.
2. HEAT TO 491K (425°F).
3. HOLD AT 491K (425°F) FOR 30 MINUTES.
4. COOL TO LESS THAN 339K (150°F) BEFORE RELEASING VACUUM.

Figure 11. Typical (a) vacuum bag layup and (b) staging conditions for Celion 6000/LARC-160 composite fabrication.

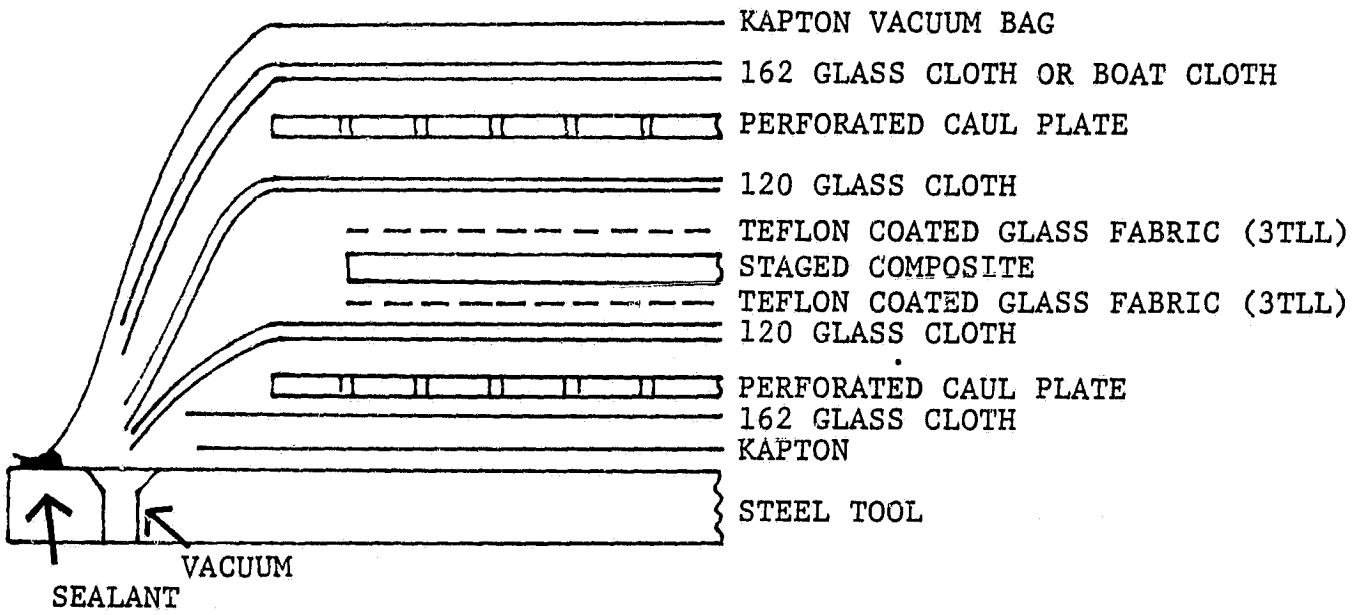

Figure 12. Vacuum bag layup for cure process of Celion 6000/LARC-160 composite.

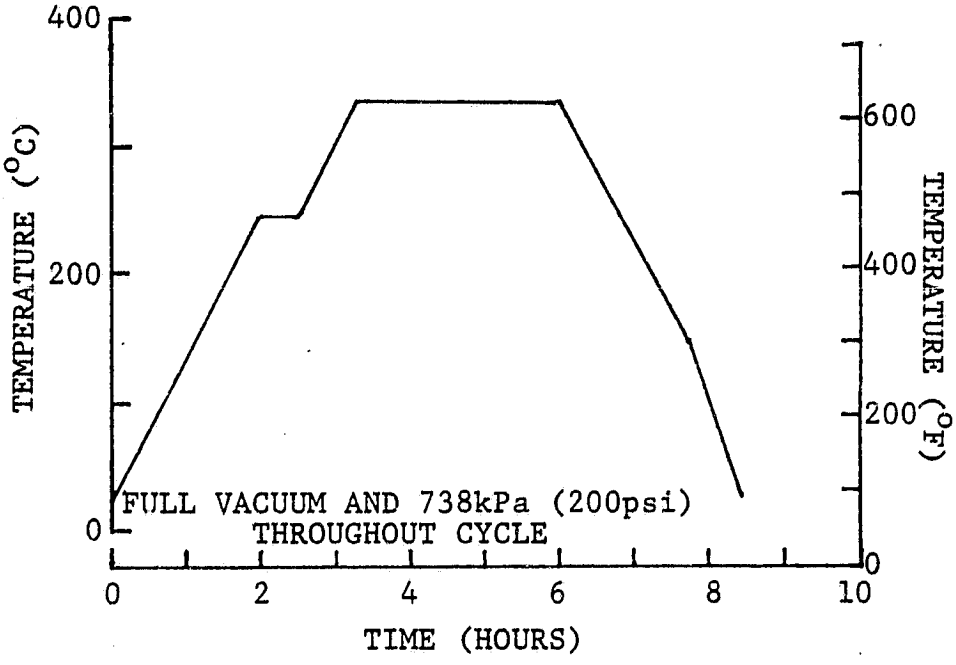

Figure 13. Final cure cycle for Celion 6000/LARC-160 Composite.

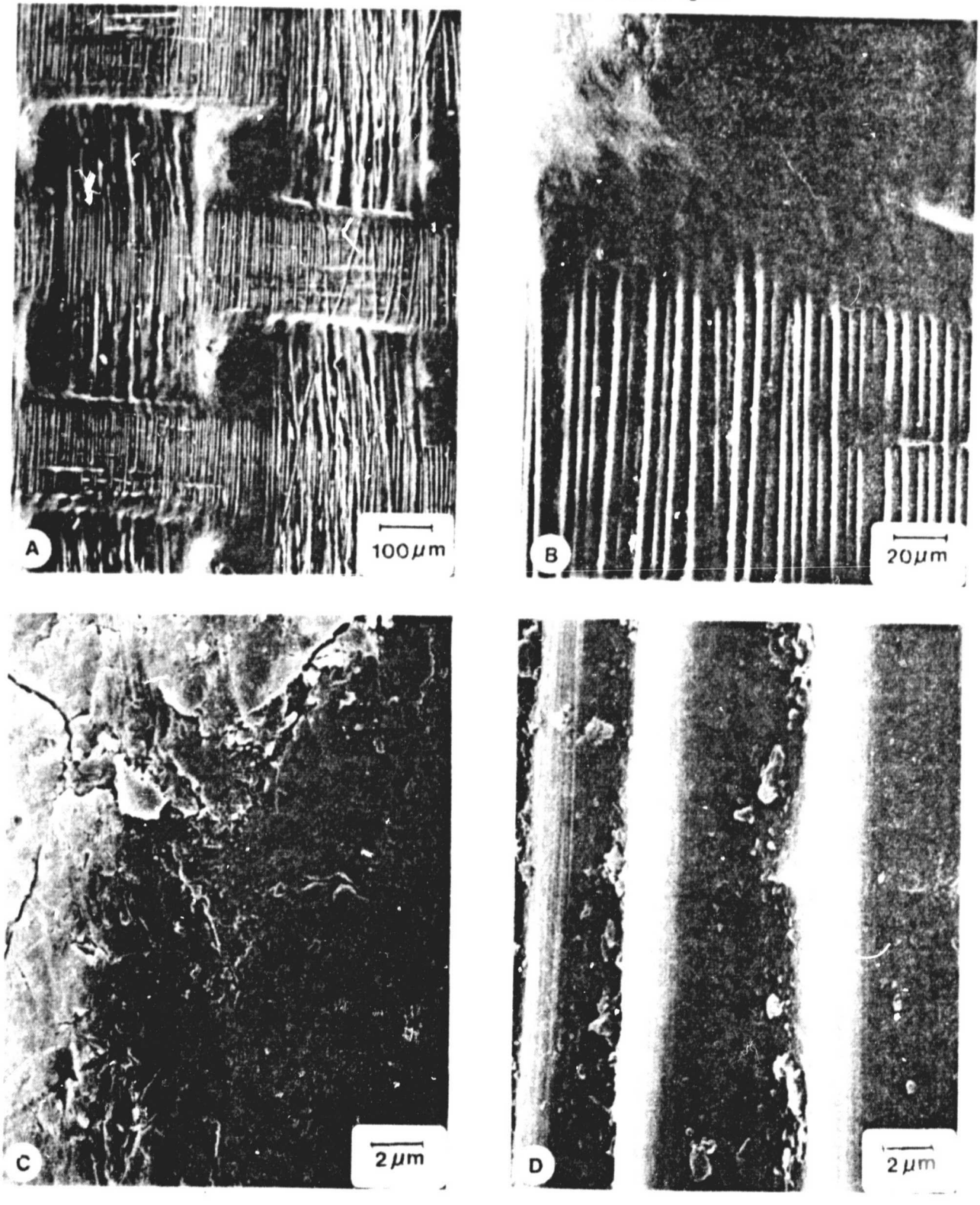

Figure 14. SEM photomicrograph of as-received composite.

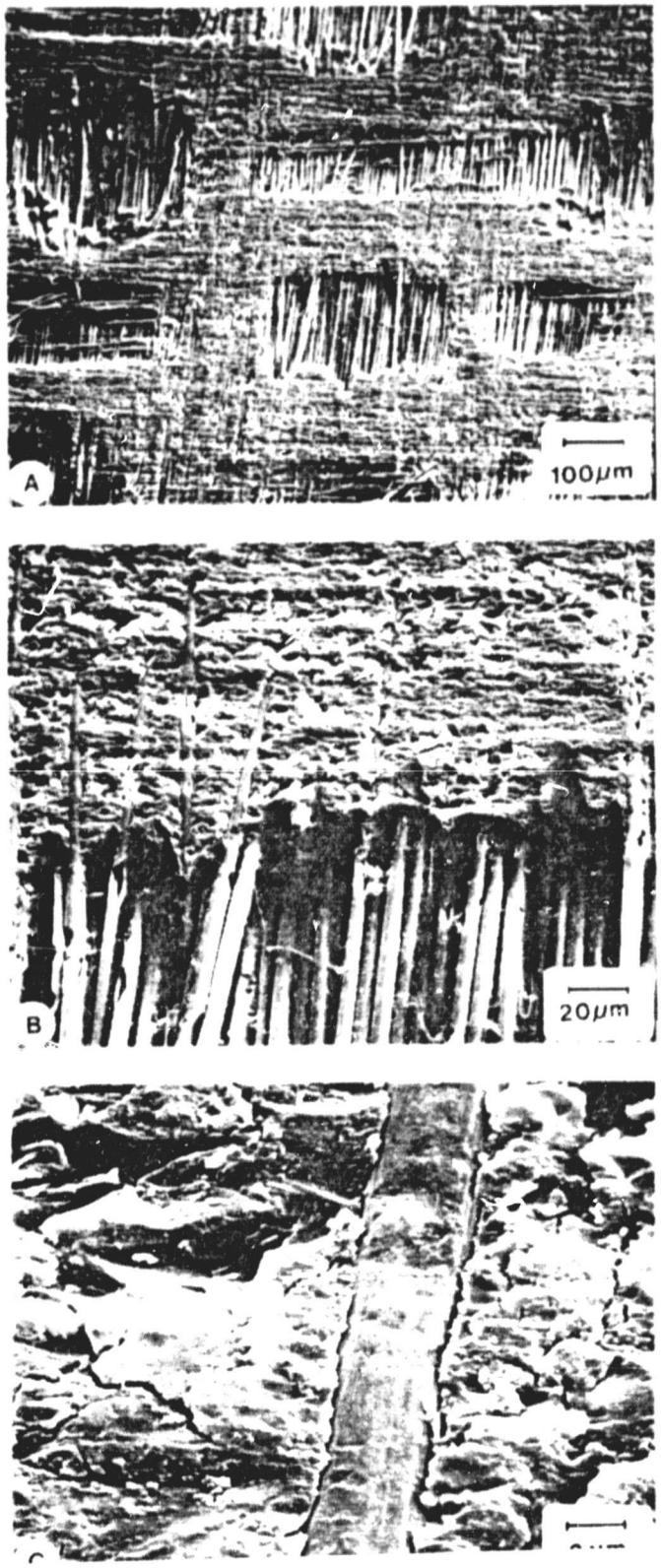

Figure 15. SEM photomicrographs of 600 SiC handsanded composite.

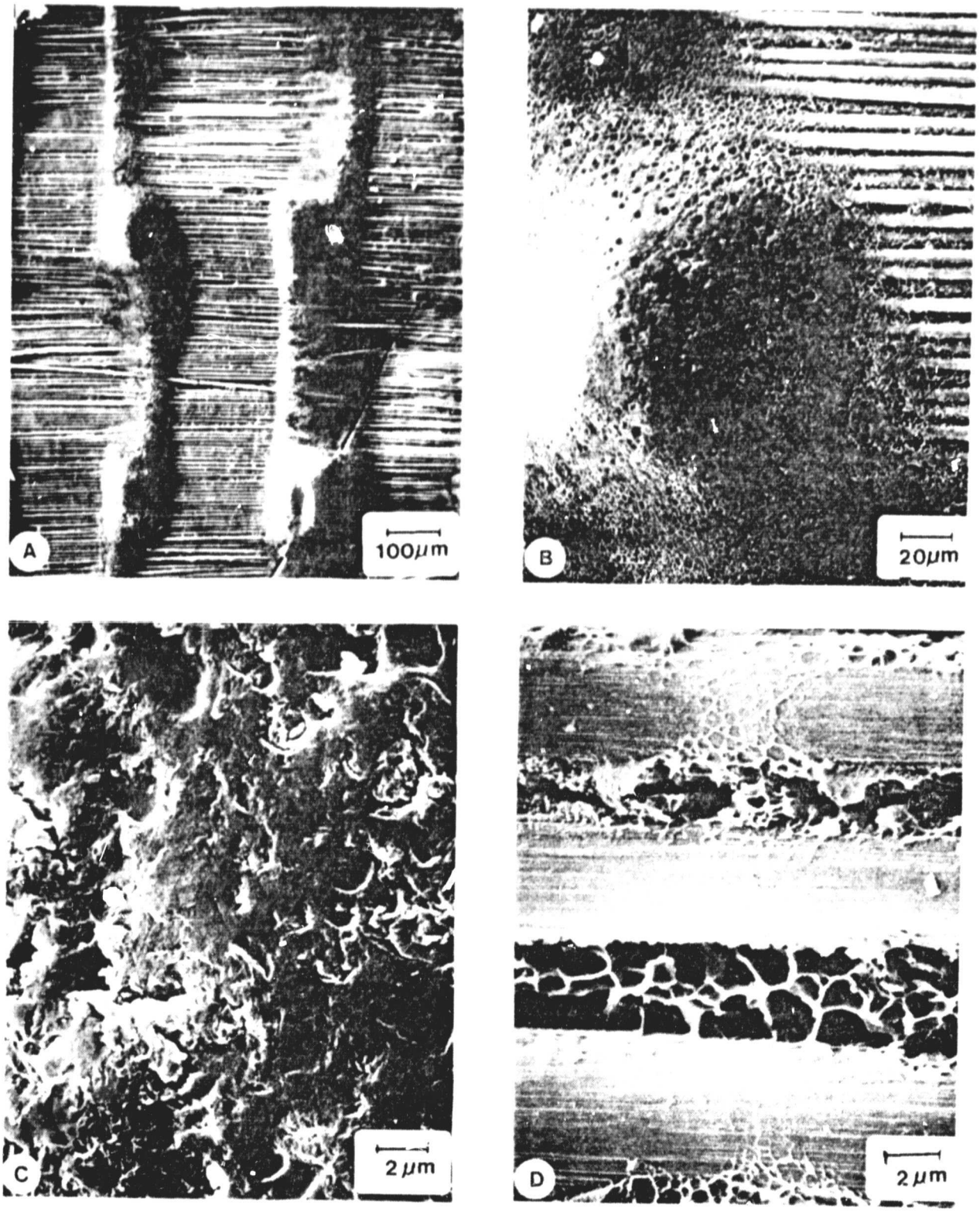

Figure 16. SEM photomicrographs of Flashblast pretreated composite.

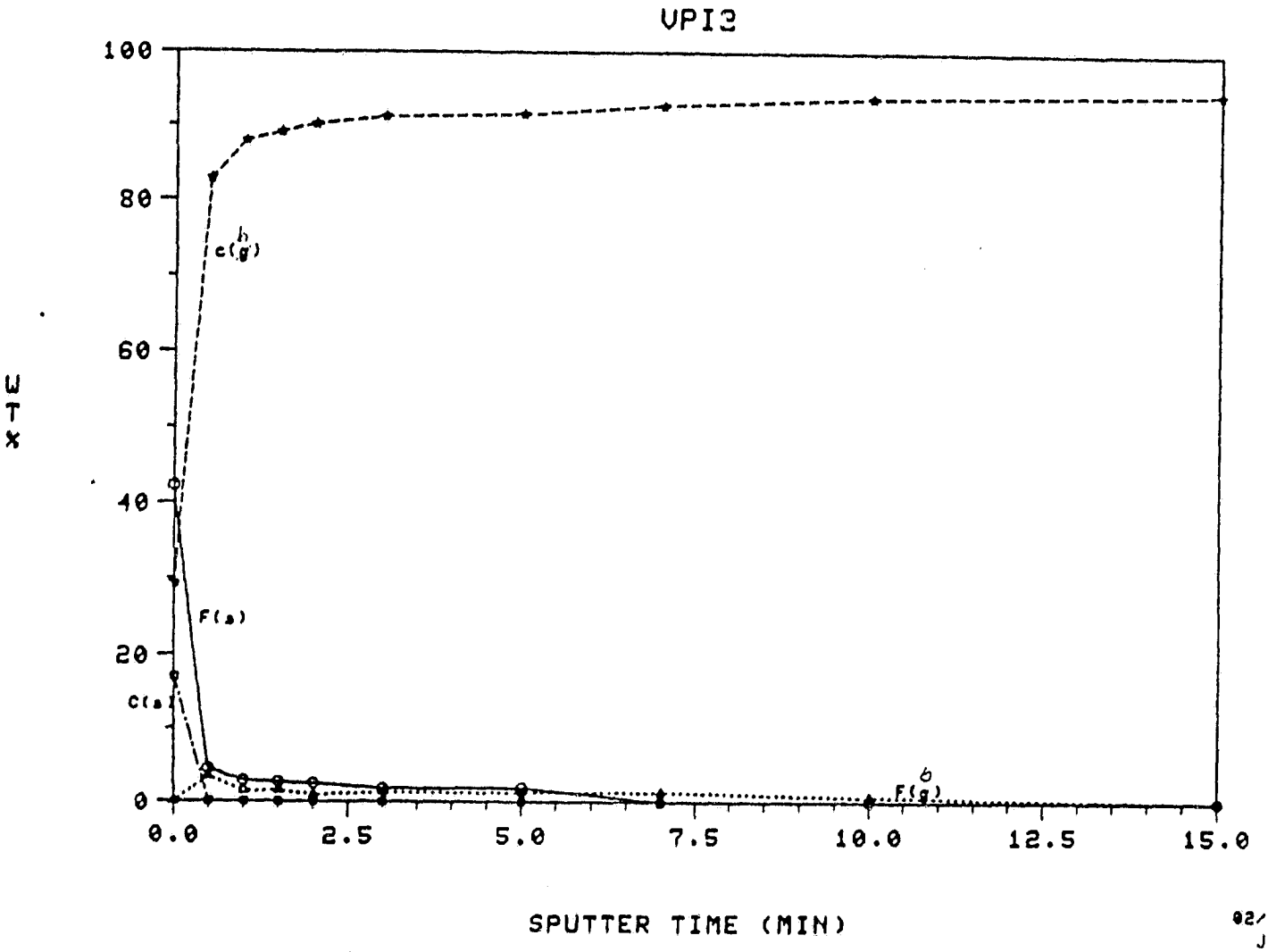

Figure 17. ESCA depth profile analysis of as-received composite.

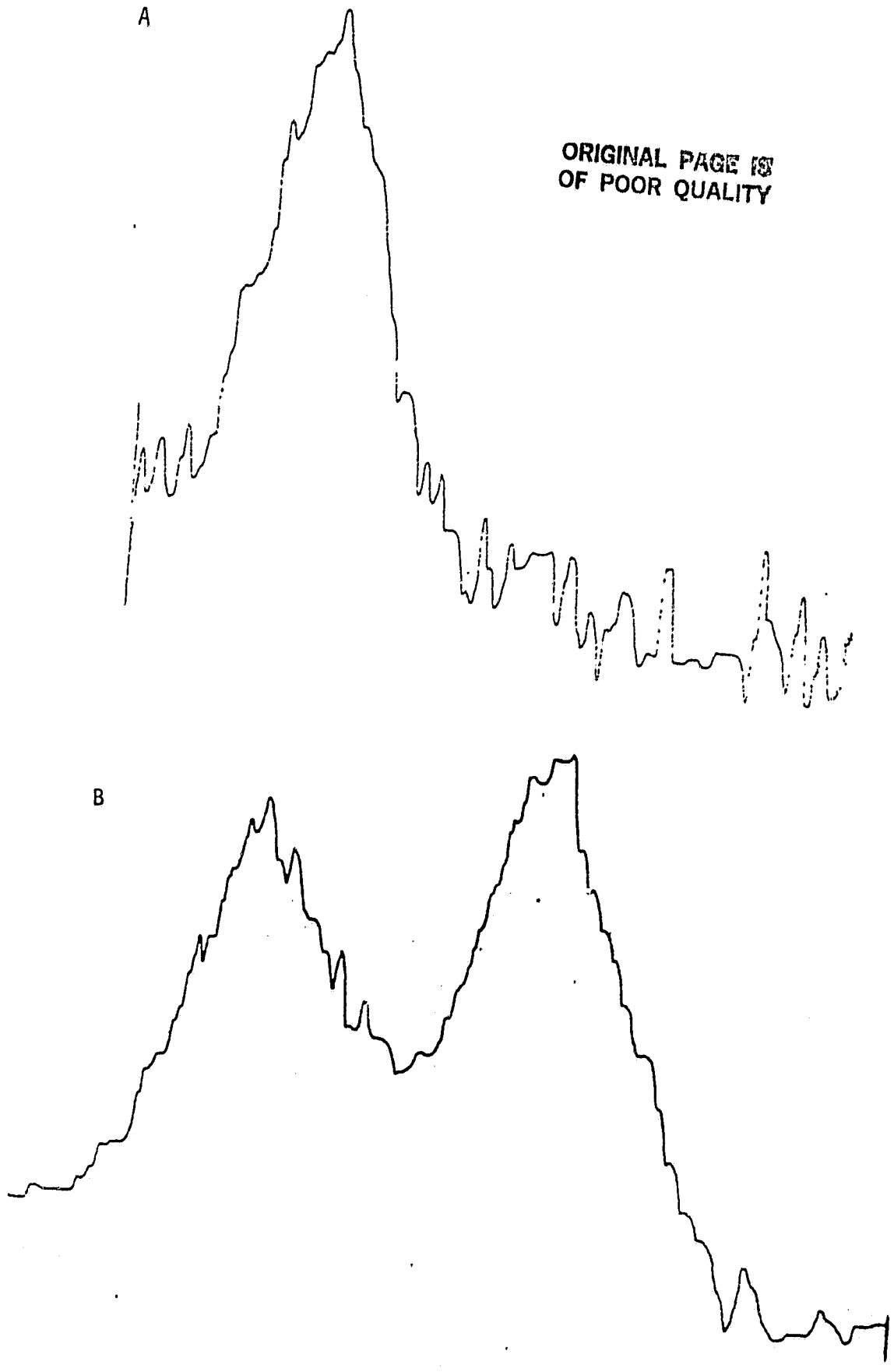

Figure 18. ESCA spectra of derivatized as-received composite.

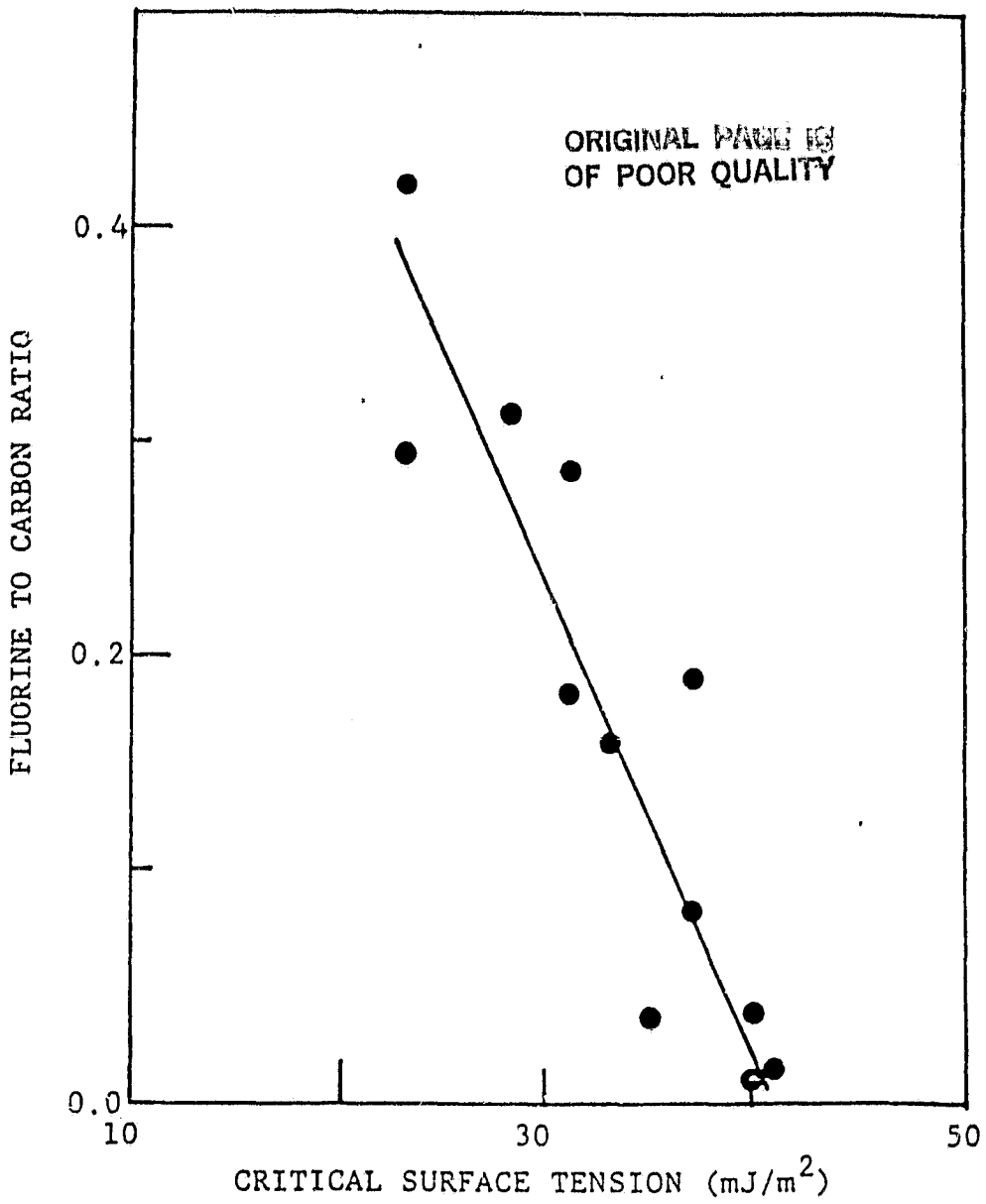

Figure 19. ESCA fluorine to carbon ratio as a function of the critical surface tension of pretreated composites.